Ultimate Strength of Reinforced Concrete Cylindrical Shells Influenced by Point Load Position

Kazuhiko MASHITA
School of Engineering, Tokai University,
1117 Kitakaname, Hiratsuka-City, Kanagawa, 259-1292, JAPAN
Phone:81-463-58-1211(Ext.4233), Fax:81-463-50-2024
E-mail:mash4233@keyaki.cc.u-tokai.ac.jp

ABSTRACT

The main purpose of this paper is to investigate, both theoretically and experimentally, the ultimate strength influenced by point load position on reinforced concrete cylindrical shells supported by pins at corners. The strength and the nonlinear mechanical characteristics of shells were studied for different load position.

The theoretical study was conducted using the material and geometrical nonlinear finite element analyses including concrete cracking and tension stiffening effects. The experimental study was conducted on reinforced micro-concrete shell specimens. One point load, which was located on either of the two different central lines on shell surface, was applied vertically on the shell surface into the final failure states.

The load level at the initial crack, the cracking patterns and the ultimate strength of reinforced concrete cylindrical shells influenced by the different position of point load are discussed based on the results of the nonlinear analysis and failure experiments.

1. INTRODUCTION

This study presents the strength of reinforced concrete shells under point load. The reinforced concrete shells have been able to show the high load carrying capacity and to cover the large space without the struts and columns. Therefore, the structural possibilities of reinforced concrete shells would be much fruitful not only as the utilization on roof structures as usual but as the other useful structures demanded on recent remarkable scientific developments. The structures covering important facilities for public use and with the double uses as both multi-purpose dome for the inner space and green park for the outer space by covering with soil and planting over there, would be proposed for the above purposes. Although in general the strength of reinforced concrete shells under uniform loading is extremely high, the strength under point load is an unknown problem.

However, there have been many problems to confirm the effective method to evaluate the strength of the reinforced concrete shell and to verify the adaptability of the nonlinear theory based on many kinds of numerical assumptions, which could be inspected by the

corresponding precise failure experiments.

The strength of the actual reinforced concrete shell is much influenced by not only the material and geometrical conditions but the boundary and loading conditions. Furthermore the strength of the numerical shell models is so much affected by the constitutive relations on material properties, the geometrical non-linearity, the idealization of the shell, the edge boundary and the shell supports and so forth.

In this study, the strength and the cracking patterns of the reinforced concrete cylindrical shells have been investigated, both theoretically and experimentally. The theoretical studies were conducted using material and geometrical nonlinear finite element analyses including concrete cracking and tension stiffening effects. Degenerate thick shell elements employing a layered discretization through the thickness were adopted. The experimental study was conducted on small-scaled reinforced micro-concrete specimens, which were loaded perpendicularly with point load on the upper shell surface up to the final failure states. The load levels at the initial crack, ultimate load carrying capacities and cracking patterns were investigated. The experimental ultimate strengths of reinforced concrete shells influences by point load position were compared with the theoretical values and discussed.

2. THEORETICAL ANALYSIS

The ultimate strengths and nonlinear behaviors of reinforced concrete shells were analyzed by material and geometrical nonlinear finite element analyses including concrete cracking and tension stiffening effects. Nine-node quadratic shell elements with a Lagrangian interpolation function were adopted with a selective integration method. A layered discretization is used to represent the concrete and steel reinforcement.

The compressive behaviors of concrete are modeled by employing a strain-hardening plasticity approach and a Drucker-Prager type yield function. A yield criterion for concrete under a bi-axial stress is considered by employing the experimental results of Kupfer (Kupfer, 1969). The crushing type of concrete fracture is a strain controlled phenomenon and a crushing condition is expressed in terms of the total strain components. The concrete ultimate compressive strain was set to be 0.003.

The tensile behaviors of concrete are evaluated by considering the effects of tension cut-off and tension stiffening. Due to bond effects for cracked concrete, a certain amount of tensile force is carried and is represented as tension stiffening. In considering these effects for cracked concrete, inverse proportional stresses from 60 percents of a concrete ultimate tensile strength to zero were evaluated within strains from zero to the concrete ultimate tensile strain equal to 0.002.

The cracked shear modulus was adopted in a smeared cracking model. The behaviors of cracked concrete are influenced much by shear stiffness, which is caused by dowel action of steel bars and aggregate interlock across the rough surfaces of cracked concrete. The cracked

shear modulus is considered by employing Cedolin's results (Cedolin, 1977).

The reinforcing steel bar is represented as a smeared layer of equivalent thickness with uni-axial strength. The elasto-plastic stress-strain relationships of the steel layers are employed by a bilinear idealization.

A geometrically nonlinear analysis is carried out using a Total Lagrangian approach for the degenerate iso-parametric shell elements.

Each reinforced micro-concrete model is a roof-type circular cylindrical shell as shown in Fig.1 and Table1. The model has the same square plan, the dimension of which is 1,120 mm (=L1) x 1,120 mm (=L3), where L1 is a shell chord-width and L3 is a shell length. The design shell thickness is 8 mm (=T0) and the rise to chord-width ratio is 1/5. The radius of curvature on the shell is 812 mm (=R). The semi-central angle is 43.54 degrees. The width and depth of edge beam and edge arch are 40 mm, respectively. These forms and dimensions of a shell were adopted taking into account of the concrete shell models in the Authors' previous study (Mashita, 1997). The loading condition is one point load, which is perpendicularly loaded in either of central line on the upper shell surface.

The shell model was corner-supported by pins, which restrain the thrust movements of edge arches. The steel reinforcement was based on the failure experiment. In a shell, it was assumed to be reinforced with 1.2mm diameter mild steel wires placed at 20 mm centers both ways. In edge member, such as edge beam and edge arch, it was assumed to be reinforced with two 3 mm diameter deformed bars placed in two layers for the depth 40 mm and with 0.85 mm diameter mild steel stirrups placed at 20 mm centers. The material constants of steel bars and wires are listed in Table 2.

Numerical study was conducted on two different types of small-scaled shells. One is a

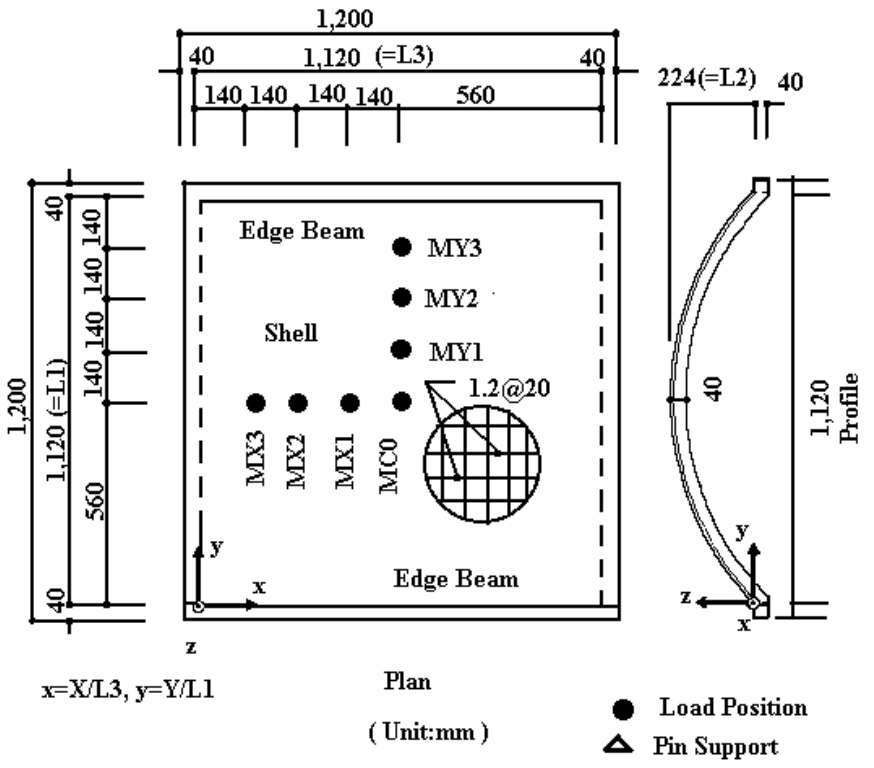

standard model and the other is an experimental model. The initial letter in the former is ‘M’ specified with a design shell thickness 8mm and the standard material properties in this study. The initial letter in the latter is ‘S’ specified with an actual shell thickness and the material properties corresponding with each failure experiment.

Fig. 1 Shell Model

Table 1 Shell Model

Type	Model	Load Position		Thick-ness T (mm)	Concrete			
		x	y		Young’s E (GPa)	Fc (MPa)	Ft (MPa)	Poisson’s Ratio
MC0	FEM	0.500	0.500	8.00	20.6	49.0	4.90	0.167
MX1	FEM	0.375	0.500	8.00	20.6	49.0	4.90	0.167
MX2	FEM	0.250	0.500	8.00	20.6	49.0	4.90	0.167
MX3	FEM	0.125	0.500	8.00	20.6	49.0	4.90	0.167
MY1	FEM	0.500	0.675	8.00	20.6	49.0	4.90	0.167
MY2	FEM	0.500	0.750	8.00	20.6	49.0	4.90	0.167
MY3	FEM	0.500	0.825	8.00	20.6	49.0	4.90	0.167
TC0	Exp.	0.500	0.500	8.72	23.6	56.3	3.00	0.240
TX2	Exp.	0.250	0.500	8.32	30.2	68.0	3.99	0.241
TY2	Exp.	0.500	0.750	9.44	30.2	68.0	3.99	0.241
SC0	FEM	0.500	0.500	8.72	23.6	56.3	3.00	0.240
SX2	FEM	0.250	0.500	8.32	30.2	68.0	3.99	0.241
SY2	FEM	0.500	0.750	9.44	30.2	68.0	3.99	0.241

Table 2 Material Constants of Steel Bar

Steel Bar(mm)	Young's E (GPa)	Yield Strength(MPa)	Ultimate Strength(MPa)
0.85	186	162	250
1.2	235	364	468
D3	198	334	487

The second letters ‘X’ and ‘Y’ in each model show the direction of the eccentrically loaded position on the upper shell surface. However, the letter ‘C’ shows the central load position. The third number shows the distance block from the central point on the upper shell surface, where one block shows a quarter of shell half-length in a projected horizontal plane.

The finite element idealizations are as follows. The concrete shell thickness is divided into 10 layers of equal thickness. The cylindrical shell surface is divided with two steps. At the first step, the whole shell surface is divided using 8 x 8 meshes of equal length in the horizontal plane, and at the second step the element applied with the point load is subdivided with 2 x 2 sub-divisions. The subdivisions of the edge arches and edge beams correspond to those of shell surface.

3. EXPERIMENTAL STUDY

The experimental failure study was conducted on 3 reinforced micro-concrete small-scaled specimens, which were listed in Table 1. The plans and dimensions of shell specimens are the

same as those stated above in the theoretical study. The initial letter ‘T’ in these specimens shows the experiment. The second and third letters in the specimens show the direction of the load position. The specimen TX2 was applied with point load eccentrically in the x direction and the specimen TY2 was applied with point load eccentrically in the y direction, while the specimen TC0 was applied with point load at the center of shell surface.

The boundary conditions in shell specimens were stiffened with edge beams and edge arches with 40mm depth and 40 mm width. The supporting conditions in shell specimens were restrained by pins at the four corners intersecting with edge beams and edge arches by restraining the thrust movement of edge arches. The reinforcement in a shell was arranged with 1.2mm diameter mild steel wires placed at 20mm centers both ways. The reinforcement in the edge members was arranged with two 3mm diameter deformed bars placed in two layers for the depth 40mm and with 0.85mm diameter mild steel stirrups placed at 20mm centers.

The actual shell thickness and material constants of concrete are listed in Table 1. The average actual shell thickness was obtained by measuring 64 points at each shell surface. The range of actual shell thickness were 7.60 to 10.40mm at TC0, 6.55 to 10.00mm at TX2 and 6.95 to 11.55mm at TY2. The standard deviations in the actual shell thickness were 0.93mm at TC0, 0.82mm at TX2 and 1.18mm at TY2. The thickness at TY2 became rather thick. The material properties at TX2 were identical with those properties at TY2, because the casting of these two specimens was done simultaneously in one batch of concrete. The material constants of concrete at TC0 were comparatively lower than those constants at TX2 and TY2.

The shell specimen was loaded perpendicularly with one point load on the upper shell surface up to the final failure states. A circular rubber plate with 5mm thickness and 50mm diameter was inserted into the contact region between the point load and the top shell surface.

4. INVESTIGATIONS

As the results of the nonlinear numerical analysis, the initial cracking load was listed in Table 3. Each value was obtained by normalizing with the load intensity of the ultimate load (Po=2.55kN) at MCO, which was a standard type with the design shell thickness and the standard material properties.

Table 3 Load Ratio at the Initial Crack to the Ultimate Load of MC0 (2.55 kN)

Type	Shell		Edge Arch				Edge Beam			
	Top	Bot	Top	Bot	Out	In	Top	Bot	Out	In
MC0	0.38	0.23	-	-	-	-	-	-	-	-
MX1	0.38	0.23	-	-	-	-	-	-	-	-
MX2	0.42	0.23	-	0.92	0.92	0.92	-	-	-	-
MX3	0.38	0.23	1.00	0.85	0.85	0.88	-	-	-	-
MY1	0.38	0.23	0.46	0.35	0.38	0.35	0.92	-	0.88	0.92

MY2	0.42	0.23	-	-	-	-	0.83	1.00	0.81	0.92
MY3	0.46	0.27	-	0.88	0.92	0.88	0.54	0.46	0.46	0.46
TC0	0.85	0.88	0.96	-	0.77	0.92	0.85	-	0.85	-
TX2	0.85	0.92	-	-	0.97	-	-	-	-	-
TY2	0.69	0.61	-	-	-	-	-	-	-	-
SC0	0.46	0.15	-	-	-	-	-	-	-	-
SX2	0.54	0.19	0.96	0.85	0.85	0.96	-	0.96	0.96	0.96
SY2	0.61	0.23	1.19	1.04	1.04	1.15	0.73	0.81	0.73	0.77

In this table, the initial cracking load intensities on the top and bottom shell surfaces, and the top, bottom, outside and inside edge member surfaces were listed. By comparing the top shell surface to the bottom shell surface as listed in this table, the initial cracks were governing on the bottom shell surface in all the numerical models. Concerning the numerical models MX1, MX2 and MX3 with the eccentric point load on the central line parallel to the x direction, there is no crack on each surface of edge beams. It is confirmed that the initial crack load intensity on each surface of edge arches decreases, as the position of point load approaches to the edge arch. As for the numerical models MY1, MY2 and MY3 with the eccentric point load on the central line parallel to the y direction, cracks on each surface of edge beams occur except for the bottom surface of edge beam at MY1. It is also confirmed that the initial crack load intensity decreases, as the position of point load approaches to the edge beam. The initial crack load intensity of a shell specimen during the failure test was hardly recognized, because the crack observations were not possible during short-time loading to minimize the loading time effects.

The ultimate strength was listed in Table 4. The ratio of each ultimate strength to the ultimate strength 2.55 kN at the numerical model MC0 and the initial crack load to each ultimate strength are listed in this table.

Table 4 Total Load Intensities until Failure

Type	Ultimate Strength Ratio to 2.55 kN at MC0	The Initial Crack Load Ratio to Ultimate Strength	
		Shell	Edge
MC0	1.00	0.23	-
MX1	1.00	0.23	-
MX2	0.96	0.24	0.96
MX3	1.11	0.21	0.76
MY1	0.96	0.24	0.36
MY2	1.04	0.22	0.81
MY3	0.96	0.28	0.48
TC0	0.96	0.88	0.80
TX2	0.97	0.47	1.00
TY2	1.16	0.53	-
SC0	0.92	0.17	-
SX2	0.97	0.19	0.85
SY2	1.23	0.19	0.59

By comparing with the ultimate strength on the standard numerical models MX1, MX2 and MX3 applied with the x-eccentric point load, the strength at MX1 is nearly equal to that at MC0, where the point load is carried on the central point on shell surface. It is pointed out that the ultimate strength of MX3 with point load adjacent to the edge arch increases, although the ultimate strength of MX2 decreases by comparing with that of MX1. By comparing the ultimate strength on the standard numerical models MY1, MY2 and MY3 applied with the y-eccentric point load, the strength at MY1 and MY3 is a little bit lower than that at MC0. However the ultimate strength of MY2 became higher. As for the standard numerical models with the design shell thickness and the standard material properties of concrete without the effects of discrepancies among thickness and material properties, the ultimate strength influenced by point load position is limited within the range of minus 4 percents to plus 11 percents. The initial crack load intensities on the shell surface at all standard numerical models occur within the range of 21 percents to 28 percents of the ultimate strength. The initial crack load intensities on edge member surface at the standard numerical models, MX1, MX2 and MX3, decrease as the point load position approaches to the edge arch.

In comparison of the ultimate strengths at the failure experimental specimens with those at the corresponding numerical models, the ultimate strength ratios, TX2/SX2 = 0.97/0.97=1.00, and TY2/SY2=1.16/1.28=0.94 were obtained, and therefore the errors in these ratios make minus 6 percents to zero percent. The agreement of the ultimate strength between the experimental results and the nonlinear numerical results is rather good. Comparing the ultimate strengths of TX2 and TY2 to that of TC0, the ratios TX2/TC0=0.97/0.96=1.01 and TY2/TC0=1.16/0.96=1.21 were obtained. Therefore it is clear that the ultimate strength under point load eccentrically applied in the x direction is lower than that eccentrically applied in the y direction. The same results were also shown among the corresponding numerical results, where the ratios SX2/SC0=0.97/0.92=1.05 and SY2/SC0=1.23/0.92=1.34 were obtained. It was reported in our previous paper (Mashita, 1997) that the effects of the small differences among concrete material properties and also a little bit differences in the actual shell thickness influence greatly the ultimate strength of the concrete shell. Therefore with this same reason, a direct comparison of the strength on the standard numerical models to that on the numerical models corresponding with the failure experimental specimens is rather difficult.

The load - vertical displacement curves at the position applied with the point load are shown in Fig.2. In this figure, the experimental and the corresponding numerical results are compared each other. As for the model MX2 applied with point load eccentrically loaded in the x direction, the numerical result shows a good agreement with the experimental one. However the result by the numerical model MY2 under the point load eccentrically in the y direction denotes the difference with the experimental result. The reason for this discrepancy would be due to the fact that the experimental test results were affected by the additional restraint caused by the horizontal force induced with keeping the loading direction perpendicularly. The position applied with point load was obliged to set to be inclined in the y direction and therefore it was

necessary for the point load to keep perpendicularly by adding the increasing horizontal reaction.

The cracking patterns in the failure experiments compared with the corresponding nonlinear numerical analyses were shown in Fig.3. On both the top and bottom shell surfaces shown in Figs. (a) and (b), cracks with a concentric circle and radial directions including the point load position occur in the experimental failure results.

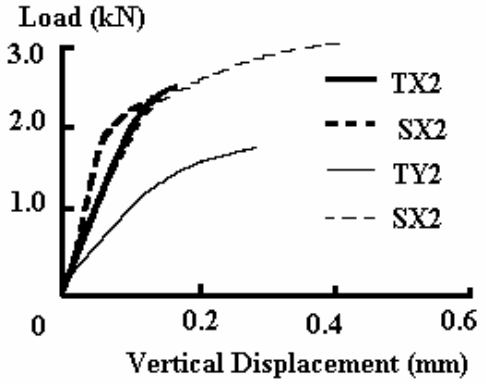

Fig. 2 Load vs. Displacement at point load position

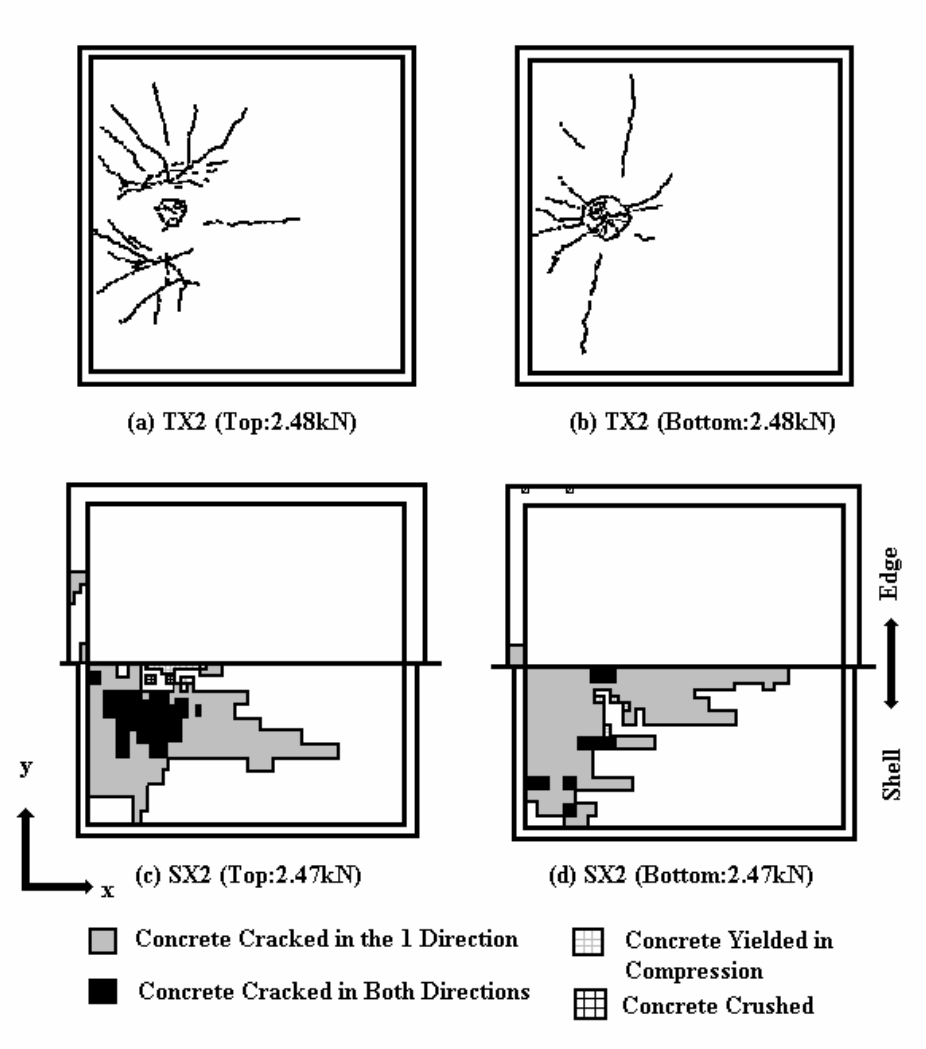

Fig. 3 Cracking Pattern

These behaviors are also recognized in the corresponding nonlinear numerical analysis shown in Figs.(c) and (d).

5. CONCLUSIONS

Within the scope of this study on reinforced concrete cylindrical shells corner-supported by pins under one point load applied on the central line on the upper shell surface, the following conclusions are obtained.

(1) As for the standard numerical models with the design shell thickness and the standard material properties of concrete without the effects of discrepancies among thickness and material properties, the ultimate strength influenced by point load position is limited within the range of minus 4 percents to plus 11 percents.
(2) Comparing the failure experimental results with the corresponding nonlinear numerical results, the discrepancies between these ultimate strengths were limited within the range of 6 percents.
(3) By comparing the failure experimental results with the corresponding nonlinear numerical results, the cracking pattern in the failure experimental results shows a good agreement with those in the corresponding nonlinear numerical results under eccentrically applied point load in the x direction.

REFERENCES

(1) Cedolin, L., 1977, “Finite Element Studies of Shear-Critical R/C Beams”, ASCE Journal of the Engineering Mechanics Division, Vol.103, No.EM3, pp.395-410.
(2) Kupfer, H. B., 1969, “Behavior of Concrete under Biaxial Stresses”, Proceedings of American Concrete Institute, Vol.66, No.8, pp.656-666.
(3) Mashita, K., 1997, “Ultimate Strength of Reinforced Concrete Cylindrical Shells with Intermediate Supports under Concentrated Loading”, Proceedings of the IASS, Singapore, Vol.2, pp.557-556.
(4) Mashita, K., 1995, “Ultimate Strength of Reinforced Concrete Cylindrical Shells Pin-Supported with Four Corners under Concentrated Loading”, Proceedings of the IASS, Milano, Vol.1, pp.369-376.